ACADEMIA ROMÂNĂ
Revue Roumaine de Chimie
http://web.icf.ro/rrch/

Rev. Roum. Chim.,
2011, *56*(5), 501-516

Dedicated to the memory of
Dr. Henry V. Kehiaian (1929–2009)

NON-ISOTHERMAL KINETIC STUDY OF THE CONSTITUTIONAL WATER LOSS FROM 12-TUNGSTOPHOSPHORIC ACID AND SOME OF ITS ACIDIC CESIUM SALTS

Viorel SASCA,[a] Orsina VERDEŞ,[a] Livia AVRAM,[a] Alexandru POPA,[a] Paul BARVINSCHI[b] and Mircea MRACEC[c*]

[a] Institute of Chemistry Timişoara of Roumanian Academy, 24 Bd. Mihai Viteazul, RO-300223 Timişoara, Roumania
[b] West University of Timişoara, Department of Physics, 4 Bd. Vasile Parvan, RO-300223 Timişoara, Roumania
[c] "Aurel Vlaicu" University of Arad, 81 Bd. Revolutiei, RO-310130 Arad, Roumania

Received October 15, 2010

The tungstophosphoric acid, $H_3[PW_{12}O_{40}]\cdot xH_2O$ (H_3PW) is one of the catalysts of the superacid class, with a low redox character relative to other heteropolyacids based on Mo or V. Their Cs acidic salts are ones of the most known compounds with application in catalysis. This study investigates the thermal behaviour of H_3PW and its acidic Cs salts and the activation energy for constitutional water loss is measured. The main thermal decomposition processes of the $H_3PW\cdot xH_2O$ and its acidic salts, $Cs_xH_{3-x}PW\cdot yH_2O$, consist of the removal of: physical adsorbed water (especially for the salt with higher specific surface area), crystallization water and constitutional water. The crystallization water loss occurs in two steps. The first step corresponds to the loss of the water molecule bound by hydrogen weak bonds and the second one to removal of the water molecule of $H_5O_2^+$. The physical adsorbed water was removed at a temperature little lower than the temperature for the first step of crystallization water loss. The activation energy of constitutional water loss was determined using the Standard Test Method for Decomposition Kinetics by Thermogravimetry-E 1641-04. The values of activation energies for constitutional water loss are reliable and support the model of aggregates with core of Cs_3PW crystallites covered of H_3PW layers for the $Cs_xH_{3-x}PW\cdot yH_2O$ microstructure.

INTRODUCTION

The tungstophosphoric acid, $H_3[PW_{12}O_{40}]\cdot xH_2O$ (H_3PW) belongs to superacids and it is one of the known catalysts.[1,2] Its acidity can be modified by partial or total exchange of protons with an adequate counter-ion resulting a new class of heteropolycompounds named heteropolyoxometalates (HPOM) with interesting catalytic properties as a combination of properties (redox, specific surface area, acidity) which can be change in a large scale. Their blend of acidic and oxidizing properties and also their versatile structure have stimulated a lot of studies and the developments of application in the field of homogeneous and heterogeneous catalysis.[1-3] The conversion of alcohols to hydrocarbons was one of the most studied, especially ethanol conversion on the H_3PW and its acidic salts,[4-8] which stays actual as increasing production and use of bioethanol.[9] In the last time some applications in the green chemistry have been studied, as esterification of fatty acids and transesterification of triglycerides for the biofuel synthesis[8,9-12] and the substitutes for tetra ethyl lead.[13]

The design of HPCs catalysts with controlled catalytic properties has been studied in detail and some models of microstructure were proposed.[14-18]

* Corresponding author: mracec@acad-icht.tm.edu.ro

A controversy on the microstructure of HPCs with Mo or W persists but the theory advanced by Okuhara *et al*.,[15] who describe the $Cs_xH_{3-x}PW_{12}O_{40}$ ($Cs_xH_{3-x}PW$) as crystallites with a core of Cs_3PW embedded of H_3PW layers gains supporters.[8,10]

The study of the thermal decomposition of H_3PW and $Cs_xH_{3-x}PW$, especially the study of kinetics for constitutional water loss, can bring valuable information on their microstructure and also about their thermal stability in the catalytic reaction under temperature. In order to compare the thermal stability for different samples it is necessary to have reliable values of activation energy. The activation energy values calculated with the Standard Test Method for Decomposition Kinetics by Thermogravimetry are reliable and they can be used to calculate thermal endurance and an estimate of the lifetime of the compounds at a certain temperature.[19]

EXPERIMENTAL

The tungstophosphoric acid $H_3[PW_{12}O_{40}]\cdot xH_2O$ (H_3PW) was synthesized according to the methods described of J. C. Bailar[20] and M. Misono *et al.*[21] from solutions of $Na_2HPO_4\bullet 12H_2O$ and $Na_2WO_4\bullet 2H_2O$ at low pH of HCl according to the reaction:

$$12WO_4^{2-} + HPO_4^{2-} + 23H^+ \rightarrow [PW_{12}O_{40}]^{3-} + 12H_2O \quad (1)$$

The H_3PW was extracted with ethylic ether and the extract was decomposed by the air bubbling. After that, the residuum was solved in a little quantity of water and the solution was heated at 323-333 K for drying.

The salts of H_3PW were prepared by precipitation from an aqueous solution of the parent acid adding the required stoichiometric quantity of counter-ion salts as Caesium nitrate under stirring. The pH was under 1.5 during the all syntheses. The precipitates were separated by filtration. After drying at 323-333 K, the $Cs_xH_{3-x}PW$ samples were heated at 523 K in air for nitrate anion total decomposition. The water content of all prepared heteropoly compounds was determined after their keeping in air at room temperature until constant mass was reached.

The synthesized compounds were: 1.$H_3PW\cdot 6\text{-}10H_2O$, 2.$CsH_2PW\cdot 5\text{-}6H_2O$, 3.$Cs_2HPW\cdot 4\text{-}5H_2O$, 4.$Cs_{2,5}H_{0.50}PW\cdot 6\text{-}8H_2O$.

The thermal analyses were carried out on a thermoanalyzer system Mettler TGA/SDTA 851/LF/1100. The measurements were conducted in dynamic atmosphere of air (50ml/min), using the alumina plates crucibles of 150 µl. The heating rates were of 2.5, 5, 7.5 and 10 K/ min in the range of temperature 298-923 K and the mass samples were about 30 mg.

The FTIR absorption spectra were recorded with a Jasco 430 spectrometer (spectral range 4000-400 cm^{-1} range, 256 scans, and resolution 2 cm^{-1}) using KBr pellets for the all prepared heteropoly compounds at room temperature. Also, the FTIR spectra of the heteropoly compounds which were heated to 523 K, 773 K and 873 K, 1 hour, under air atmosphere, were recorded.

Powder X-ray diffraction data were obtained with a XR Fischer diffractometer using the Cu K_α radiation in the 2θ range 5-60° for the heteropoly compounds at room temperature and for heated samples at 873 K, 1 hour, under air atmosphere.

RESULTS AND DISCUSSION

The primary structure (Keggin unit structure) of all synthesized compounds was check up by the FTIR analysis, as the IR spectra are like fingerprints for the heteropoly compounds with Keggin structure. The main IR absorption bands of the Keggin Unit-KU from literature data are: ν_{as}P-O_i-W, 1080-1081; ν_{as}W-O_t, 976-995; ν_{as}W-O_c-W, 890-900; ν_{as}W-O_e-W, 805-810 cm^{-1},[22] respectively, ν_{as}P-O_i-W, 1079; -ν_{as}W-O_t, 975; ν_{as}W-O_c-W, 887; ν_{as}W-O_e-W, 795 cm^{-1} in H_3PW and ν_{as}P-O_i-W, 1080; -ν_{as}W-O_t, 985; ν_{as}W-O_c-W, 890; ν_{as}W-O_e-W, 804 cm^{-1} in $C_{2.7}H_{0.3}PW$.[23]

In the IR spectra of the H_3PW and its salts, a large band between 3000-3400 cm^{-1}, with a shoulder, is observed and it was assigned to crystallization water-hydrogen bonded and to hydrogen-bond vibrations (hydrogen-bonds formed between neighbouring KUs). The shoulder at 3355 cm^{-1} was assigned to ν(OH) of protonated water.[23,24] The others two bands in relation to water molecules vibration, the 1710-1720 cm^{-1} and the 1615 cm^{-1}, were assigned to δ vibrations of protonated water (hydroxonium ions, H_3O^+ or $H_5O_2^+$), respectively to δ vibrations of nonprotonated water molecules.[24,25]

The FT-IR analysis confirms the presence only of the specific bands of the KU in the synthesized compounds, H_3PW and its Cs salts, as can be deduced from Fig. 1a. All the characteristic bands of the KU are still observed for the samples heated at 523 K, even the bands assigned to water and hydroxonium ions (Fig. 1b). This means that the samples take water in short time from atmosphere during the procedures of samples shaping as KBr pellets. By increasing of Cs content, an increase of thermal stability was observed, thus, the primary structure was preserved until 873 K for the CsH_2PW, Cs_2HPW and $Cs_{2.5}H_{0.5}PW$ as all characteristic IR bands are still present at this temperature unlike to H_3PW (Fig. 1c).

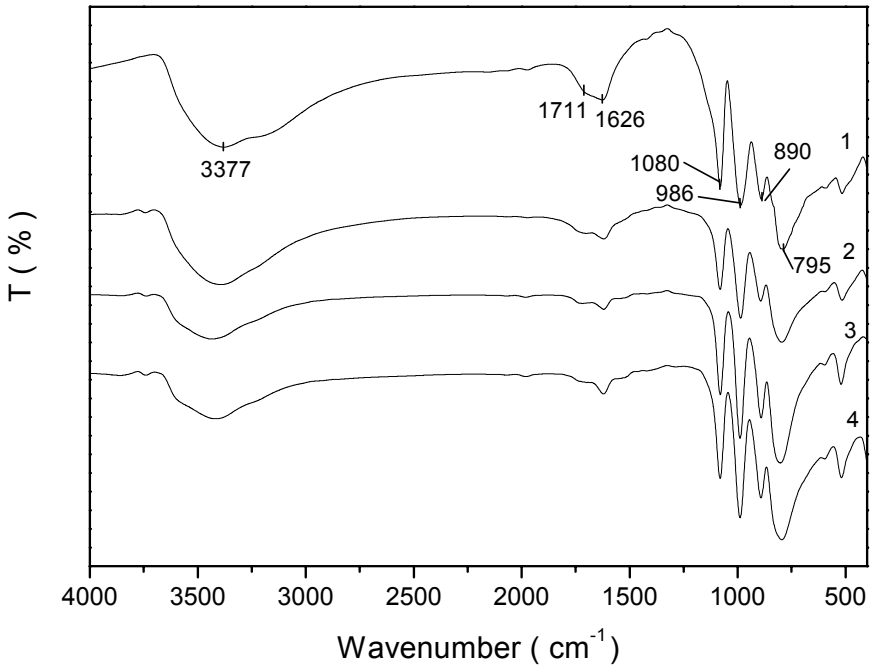
T (%)
3377
1711
1626
1080
986
890
795
1
2
3
4
4000
3500
3000
2500
2000
1500
1000
500
Wavenumber (cm-1)

a

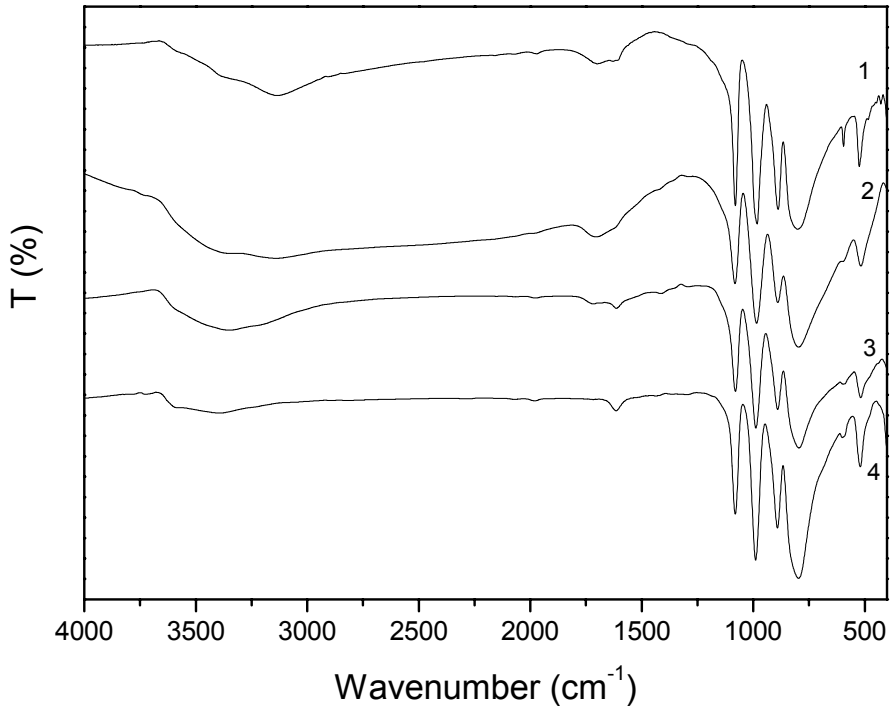
T (%)
1
2
3
4
4000
3500
3000
2500
2000
1500
1000
500
Wavenumber (cm-1)

b

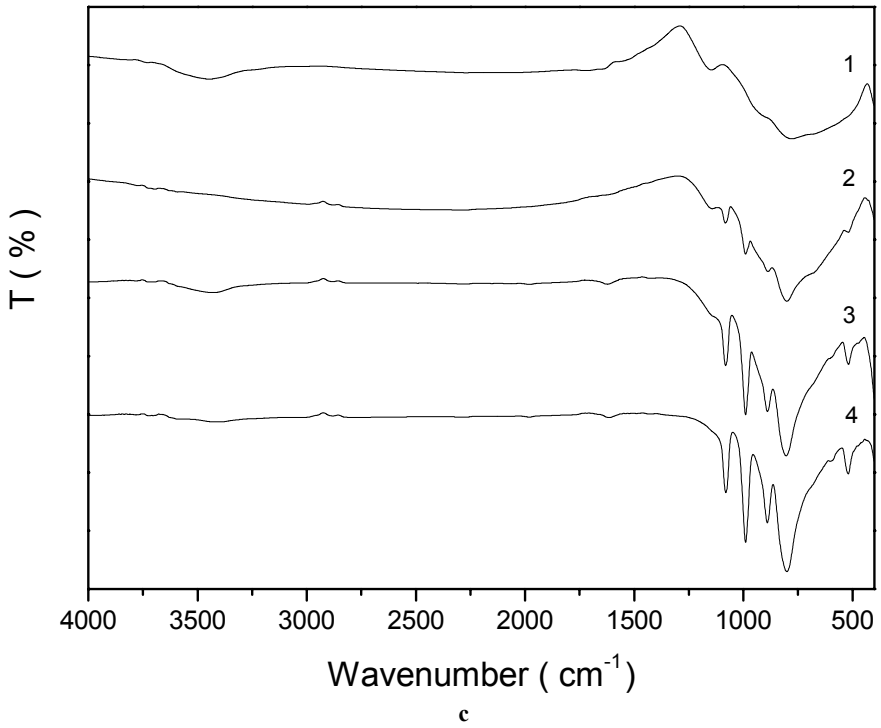

c

Fig. 1 – FTIR spectra of (1) H_3PW, (2) CsH_2PW, (3) Cs_2HPW and (4) $Cs_{2.5}H_{0.5}PW$ and:
a) fresh; b) after calcination at 573 K, 1h, in air atmosphere; c) after calcination at 873 K, 1h, in air atmosphere.

The $H_3PW{\cdot}6H_2O$ and their Cs salts have crystal structure of cubic Pn3m symmetry.[25] The X-ray diffraction spectra (Fig. 2a) of synthesized compounds exhibit all the reflections corresponding to cubic crystalline structure, similar with other literature data.[3,11,17,26,27] The X-ray diffractograms of samples heated at 873 K (Fig. 2b) confirm the TG-DTA analyses and the IR investigations: the H_3PW was decomposed completely to corresponding oxides and the WO_3 was crystallized. The spectrum 1 (Fig. 2b) is similar with literature data for cubic WO_3.[28,29] The WO_3 is present in the all acidic salts as a result of partial decomposition, as its main characteristic line (100) can be observed in their spectra with decreasing intensities with respect to Cs content increase.

The thermal decomposition of the $H_3PW{\cdot}xH_2O$ and its acid Cs salts takes place between 298 K and about 873 K. The final decomposition temperature depends on the composition and the used heating rate. Then, the thermal analysis of the $H_3PW{\cdot}xH_2O$ shows the loss of water in three steps (Fig. 3). The first one corresponds to the loss of the physical adsorbed water and the water molecule bound by hydrogen weak bonds in the temperature range of 298-383 K. The second step corresponds to the water molecules of $H_5O_2^+$ expelled in the range of 383-573 K as in the $H_3PW{\cdot}6H_2O$ all the 6 water molecules are bonded by H^+ (Fig. 3a).[25,27] The third step is the constitutional water loss, over 573 K (the water formed of the protons and the oxygen of the $[PW_{12}O_{40}]^{3-}$) (Fig.3). The water molecules bound by weak hydrogen bonds and the water molecules of $H_5O_2^+$ are considered as crystallization water. The TG-DTA experiments have shown the complete elimination of the physical adsorbed water and the crystallization water from $H_3PW{\cdot}xH_2O$ after isothermal heating at 573 K for 1 h, without the loss of constitutional water, because the mass loss corresponding to the segment 1-2 from TG curve (Fig. 3) gives very close values to the theoretical ones for the constitutional water content of all compounds.

The thermal curves of decomposition for all synthesized compounds and all heating rates, without the isothermal segments at 573 K, can be seen in Fig. 4.

The $CsH_2PW{\cdot}5H_2O$ and $Cs_2HPW{\cdot}5H_2O$ decomposition by the loss of water in three steps can be observed on TG curves and the maxima rates for these steps are evidenced on the DTG and DTA curves (endothermal peaks) as can be observed in Fig. 4b,c. In the $Cs_{2.5}H_{0.5}PW$ case, the second step (the water bonded as $H_5O_2^+$) could be observed just a shoulder on the DTG and DTA

curves and also the peaks height of constitutional water loss are diminished, as result of lower H^+ content. On the other hand, a high content of physical adsorbed water (probable water of pores, which is removed at lower temperature as the water molecules bond of H^+) was evidenced for the salts with higher specific surface area, $Cs_2HPW{\cdot}4\text{-}5H_2O$ and $Cs_{2,5}H_{0.50}PW{\cdot}6\text{-}7H_2O$ (Fig. 4c,d).

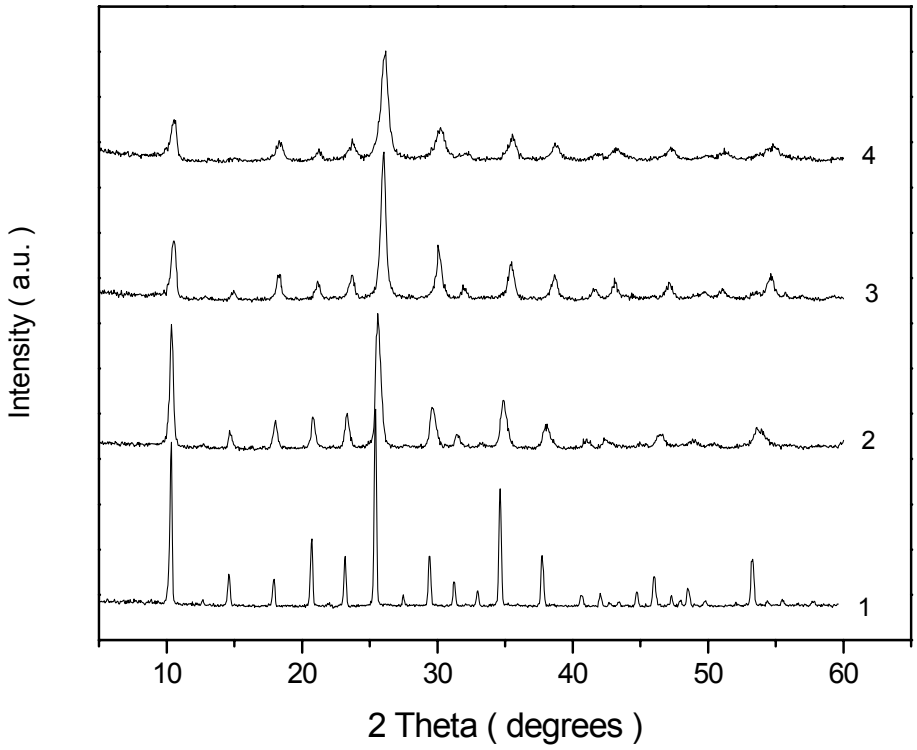

a

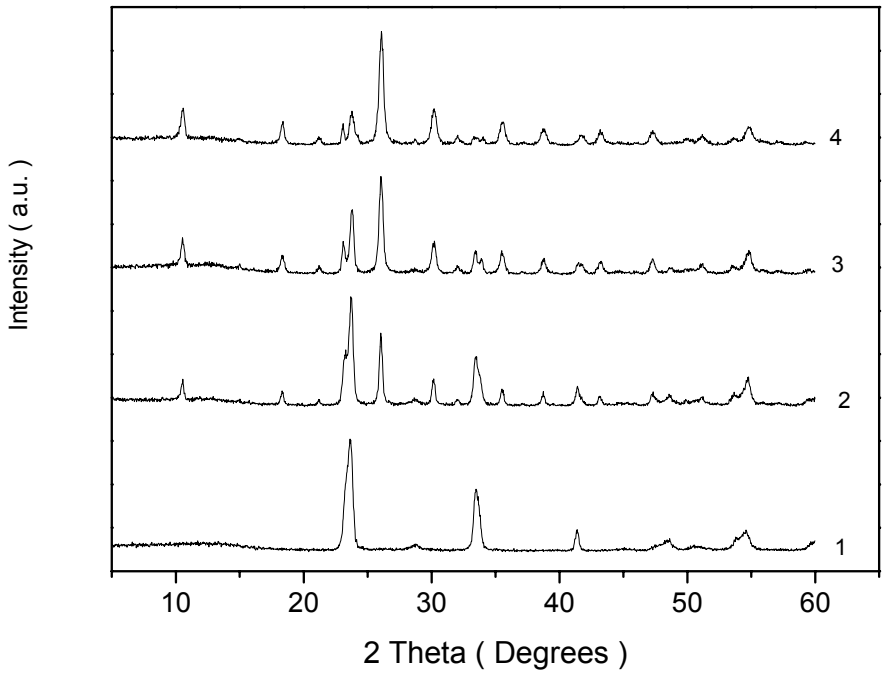

b

Fig. 2 – X-ray diffraction patterns of (1) $H_3PW{\cdot}6H_2O$, (2) $CsH_2PW{\cdot}5.6H_2O$, (3) $Cs_2HPW{\cdot}5.3H_2O$ and (4) $Cs_{2.5}H_{0.5}PW{\cdot}8.6H_2O$: a) at room temperature (up); b) after calcination at 873 K, 1h, in air atmosphere (down).

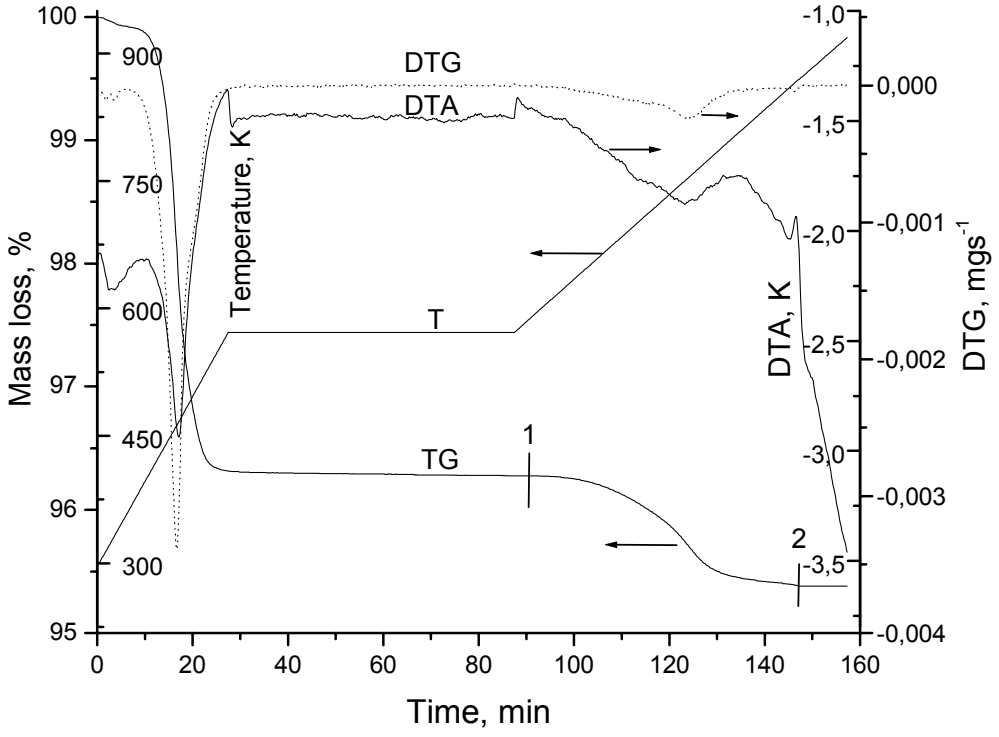

a

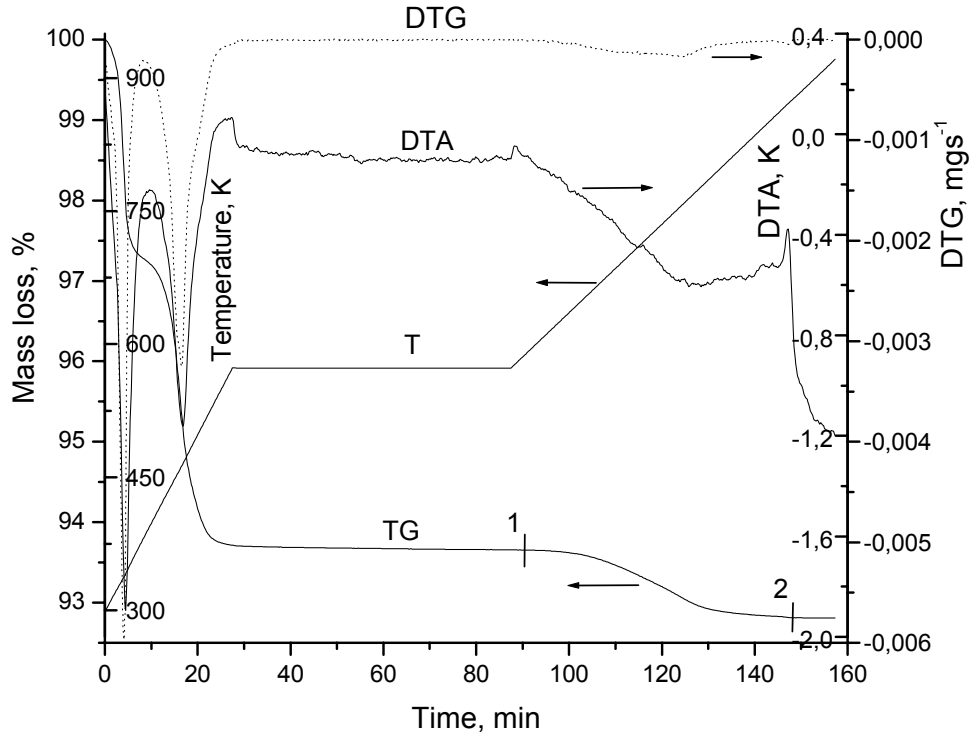

b

Fig. 3 – The thermal decomposition curves of the $H_3PW{\cdot}6H_2O$ and $H_3PW{\cdot}10H_2O$ for the heating rate of 10 K/min from 298 K to 573 K and 5 K/min from 573 K to 923 K.

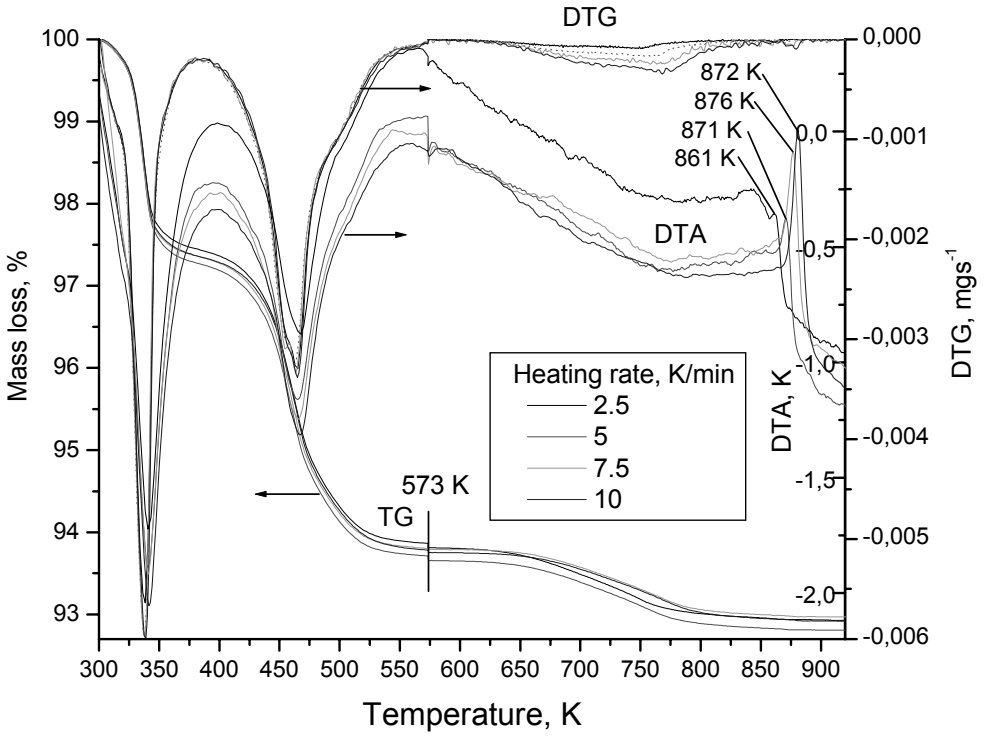
DTG
DTA
TG
872 K
876 K
871 K
861 K
573 K
Heating rate, K/min
2.5
5
7.5
10
Mass loss, %
DTG, mgs^{-1}
DTA, K
Temperature, K

a

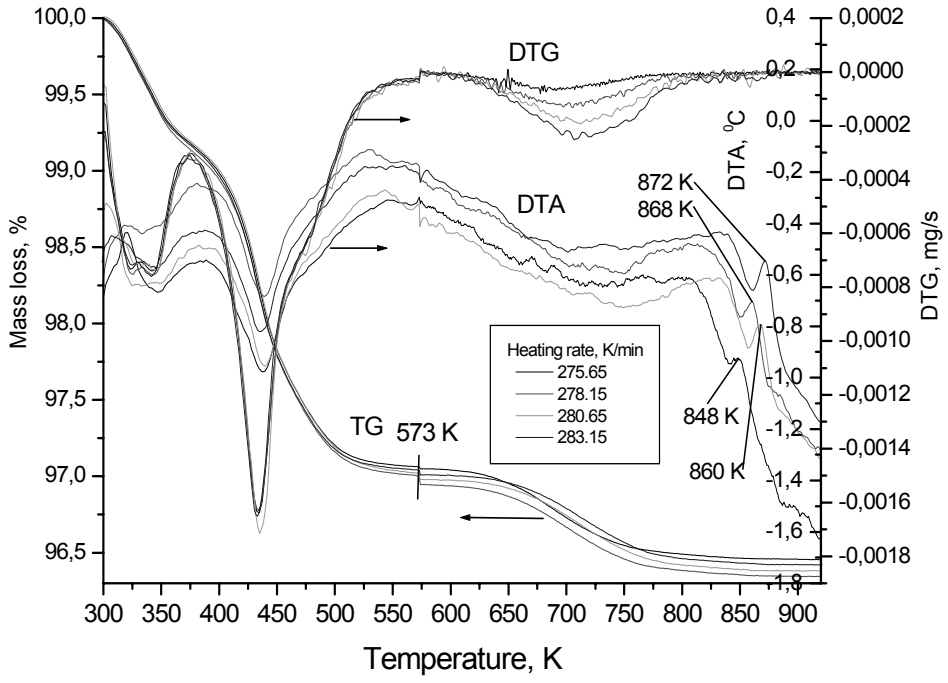
DTG
DTA
TG
872 K
868 K
848 K
860 K
573 K
Heating rate, K/min
275.65
278.15
280.65
283.15
Mass loss, %
DTG, mg/s
DTA, °C
Temperature, K

b

Fig. 4

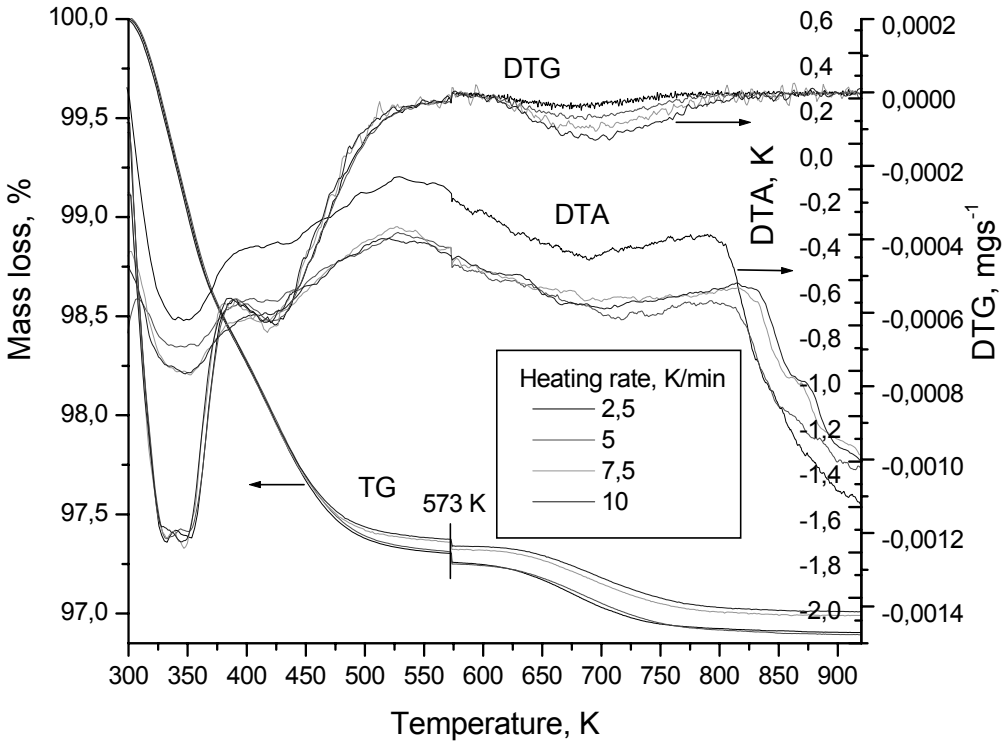

c

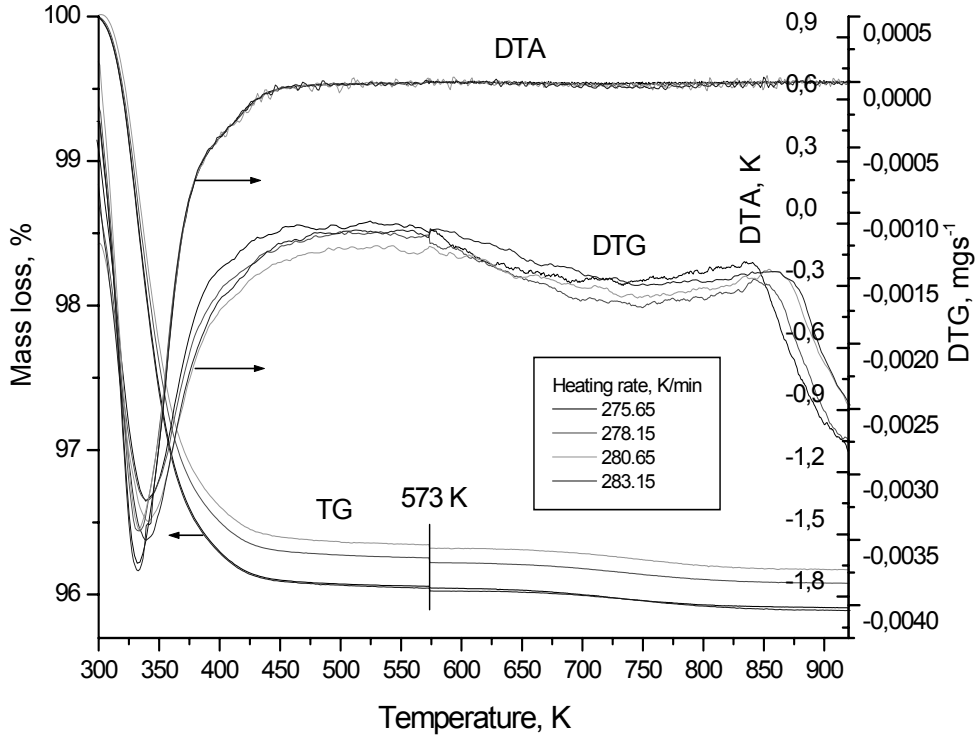

d

Fig. 4 – The thermal decomposition curves of:
a) $H_3PW{\cdot}6H_2O$, b) $CsH_2PW{\cdot}5H_2O$, c) $Cs_2HPW{\cdot}5H_2O$, d) $Cs_{2,5}H_{0.50}PW{\cdot}8H_2O$ at the heating rates of 2.5, 5, 7.5 and 10 K/min.

The final process of WO_3 crystallization gives: exothermal peaks on DTA curves for $H_3PW{\cdot}10H_2O$, and $CsH_2PW{\cdot}5H_2O$, only shoulders for $Cs_2HPW{\cdot}5H_2O$ and no thermal effect for $Cs_{2,5}H_{0.50}PW{\cdot}8H_2O$. The exothermal peak intensities increase with heating rate values, the highest being for the heating rate of 10 K/min (Fig. 4a,b,c) as the difference between the heat flow gave out by crystallization and the dissipated heat flow of samples has the highest value.

The following observations on the samples heated at 873 K are: (a) the presence of specific IR bands for KUs in the IR spectra of the all three salts and their disappearance from the $H_3PW{\cdot}6H_2O$ spectrum; (b) the presence of the reflections corresponding to cubic secondary structure of KUs arrangements, together with the characteristic reflections of WO_3 from the XRD spectra for the acidic salts and the presence of only the characteristic reflections to WO_3 in XRD spectrum of $H_3PW{\cdot}6H_2O$, support the acidic salts microstructure as mixture of acid and neutral salt in various ratios as function of Cs content. The more so as, if the $CsH_2PW{\cdot}5H_2O$, $Cs_2HPW{\cdot}5H_2O$ and $Cs_{2,5}H_{0.50}PW{\cdot}8H_2O$ are true acidic salts, their decomposition have to give lacunar Keggin structure, which have to be observed in FTIR spectra by P-O band splitting as result of lower symmetry for central atom (P) by one oxygen removal,[30] but such change was not observed in the spectra.

The acidic salts can be written down as mixture of H_3PW and Cs_3PW: $6Cs_{2.5}H_{0.5}PW=1H_3PW+5Cs_3PW$, $3Cs_2HPW=1H_3PW+2Cs_3PW$, $3CsH_2PW_{12}=2H_3PW+1Cs_3PW$ and as general formula: $Cs_xH_{3-x}PW{\cdot}yH_2O = (1-x/3)H_3PW+Cs_x[PW]_{x/3}$. All these observations lead to the conclusion that only the KUs belonging to H_3PW were decomposed to oxides in this range of temperature.

Based on these observations and on the thermal analyses results, the main decomposition processes of the $H_3PW{\cdot}6H_2O$ and the $Cs_xH_{3-x}PW{\cdot}yH_2O$ are showed in Fig. 5.

The next question is: Are the $Cs_xH_{3-x}PW{\cdot}yH_2O$ compounds a homogenous mixture of Cs_3PW and H_3PW or a heterogeneous mixture? In the last case, the heterogeneous mixture could be a mixture of H_3PW and Cs_3PW crystallites or a mixture of agglomeration of crystallites with a core of Cs_3PW crystallites covered with layers of H_3PW. The homogeneous mixture means the crystallization of Cs_3PW and H_3PW take place together, but this model can not explain the abrupt increase of the specific surface area for the content of Cs over 2/KU.[15,31]

The kinetics for constitutional water loss was studied using the Standard Test Method for Decomposition Kinetics by Thermogravimetry.[19] The segments of TG curves for non-isothermal heating from 573 K to 923 K were used for determine the absolute temperatures at constant conversion-α, for the range of constant conversion values from 5% to 95%, with the interval of 5%, as can be seen in Fig. 6a. In Figs. from 6a,b to 9a,b are shown the diagrams used for calculation of the activation energy and pre-exponential factor for all synthesized compounds.

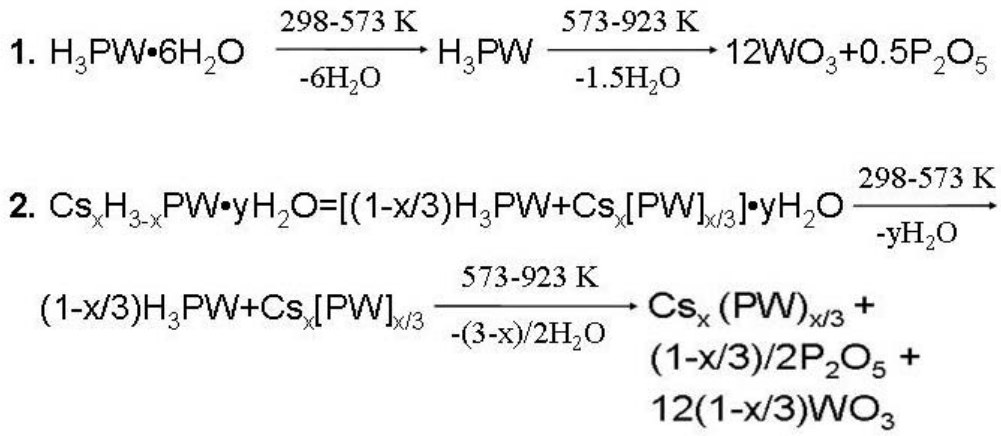

Fig. 5 – The scheme for the thermal decompositions of the $H_3PW{\cdot}6H_2O$ and $Cs_xH_{3-x}PW{\cdot}yH_2O$.

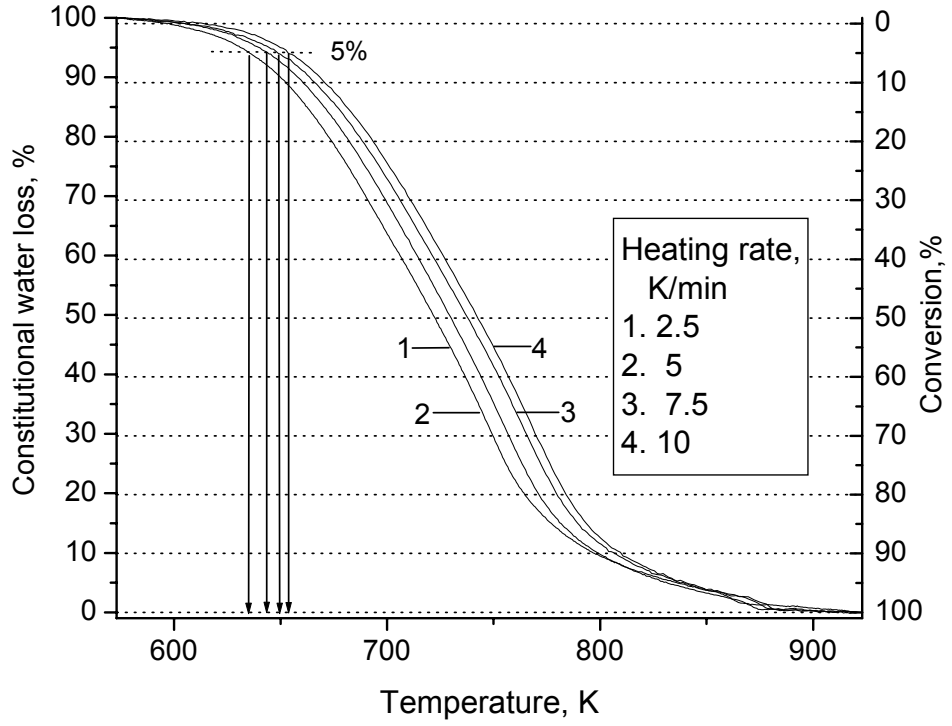

a

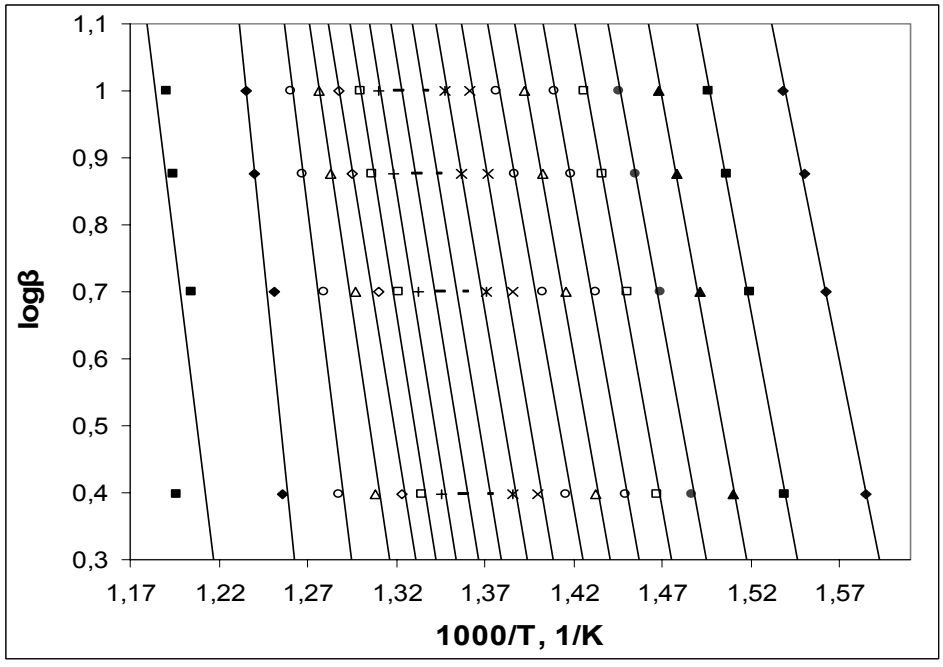

b

Fig. 6 – The constitutional water loss curves at 2.5, 5, 7.5 and 10 K/min for the H_3PW(a) and the Arrhenius plot of log(heating rate-β) function of inverse temperature (1/T) of constant conversion data (b).

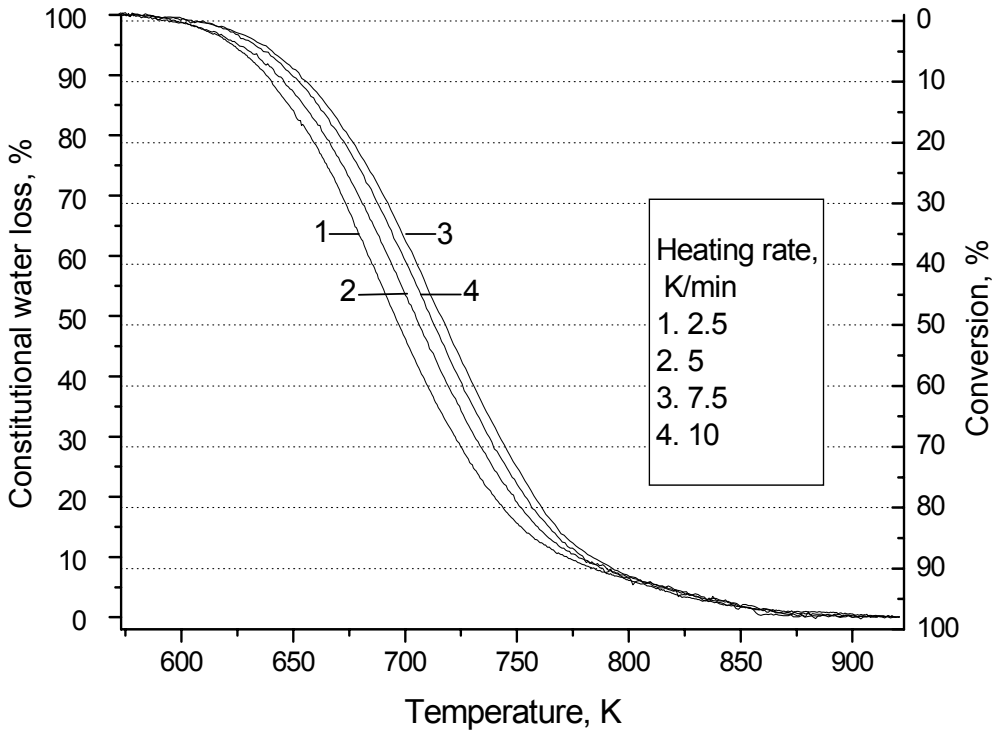

a

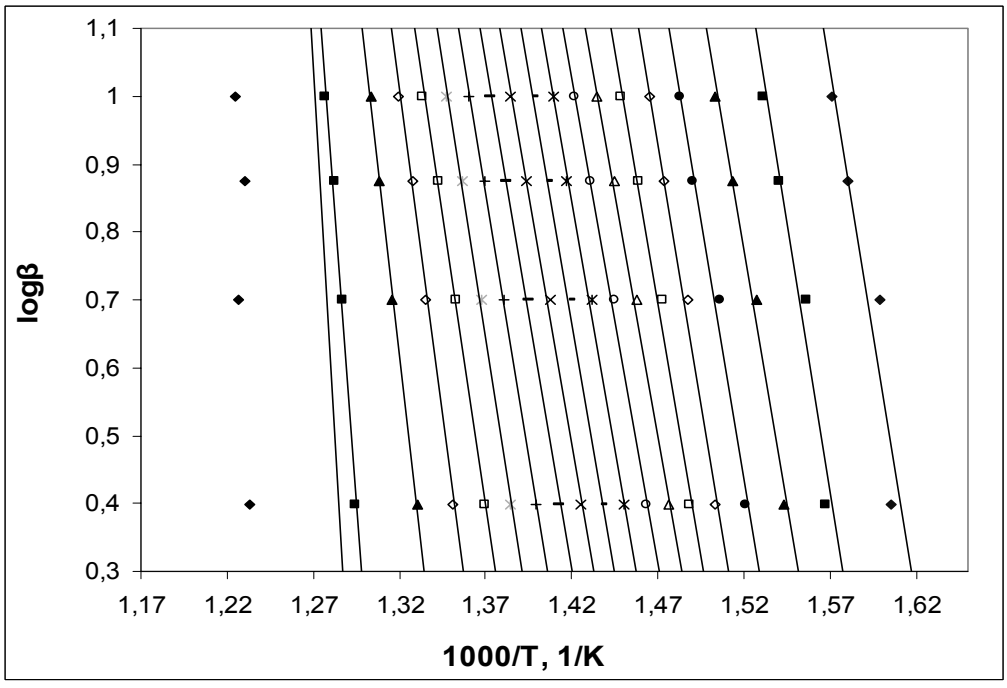

b

Fig. 7 – The constitutional water loss curves at 2.5, 5, 7.5 and 10 K/min for the Cs H_2PW(a) and the Arrhenius plot of log(heating rate-β) function of inverse temperature (1/T) of constant conversion data (b).

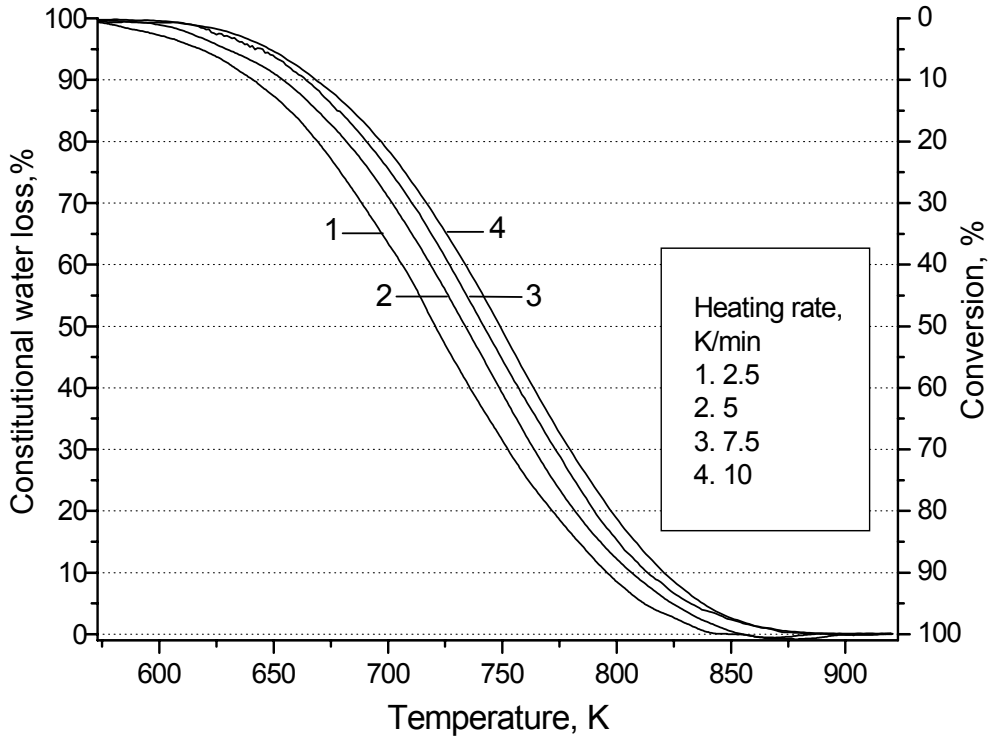

a

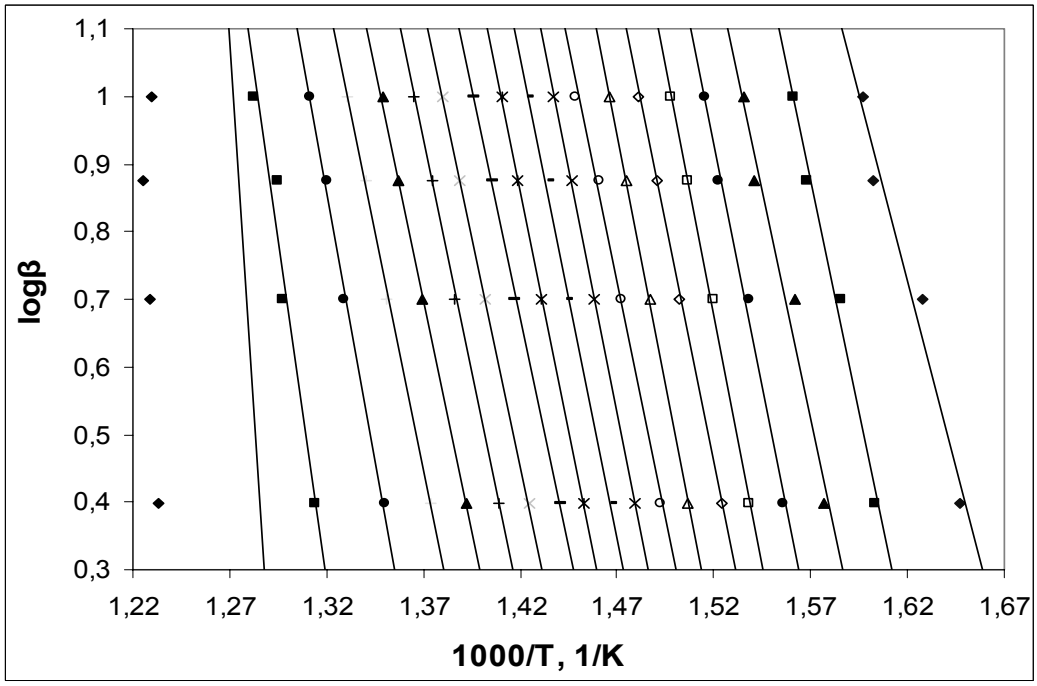

b

Fig. 8 – The constitutional water loss curves at 2.5, 5, 7.5 and 10 K/min for the Cs_2 HPW(a) and the Arrhenius plot of log(heating rate-β) function of inverse temperature (1/T) of constant conversion data (b).

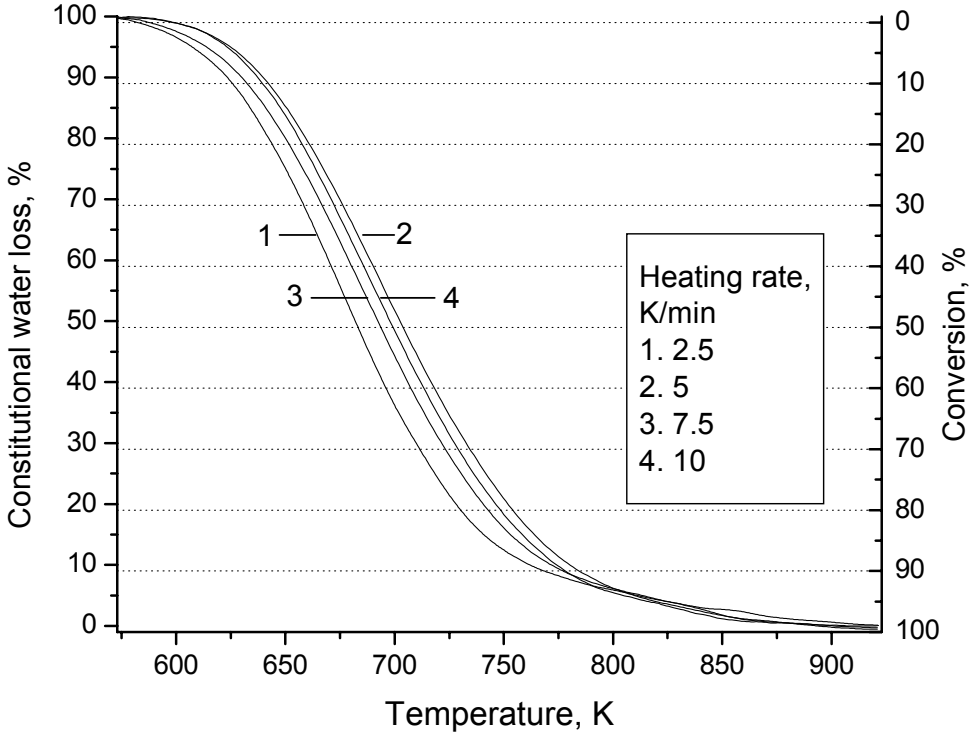

a

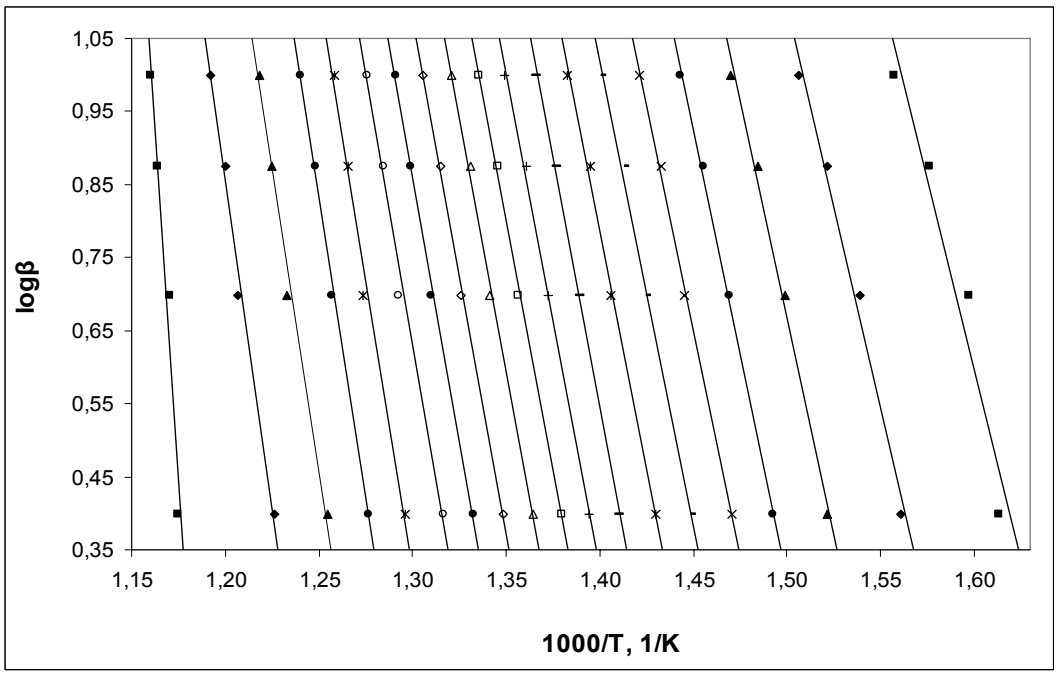

b

Fig. 9 – The constitutional water loss curves at 2.5, 5, 7.5 and 10 K/min for the $Cs_{2.5}$ $H_{0.5}PW$(a) and the Arrhenius plot of log(heating rate-β) function of inverse temperature (1/T) of constant conversion data (b).

The activation energy was calculated with the equation:[19]

$$E=-(R/b)\bullet\Delta(\log \beta)/ \Delta(1/T), \quad (1)$$

The symbols used have the following definitions:

R=gas constant, 8.314 J/(Mol·K),

b=approximation derivative, 0.457 for the first iteration,

β=heating rate, K/min,

T=temperature K) at constant conversion,

Δ(log β)/ Δ(1/T)=the slope of the Arrhenius plot for logβ function of 1/T of constant conversion data.

According to this method, the calculation of E was repeated with the new value for b selected from the Numerical Integration Constants table[19] function of the value for E/RT_c (T_c-temperature at constant conversion for the heating rate closest to the midpoint of the experimental heating rate, 5 K/min in our case) until the value for the activation energy changes by less 1%, this activation energy is named E_r.

The pre-exponential factor, A, was calculated with the equation:[19]

$$A=-(\beta'/E_r) \bullet R\bullet\ln(1- \alpha) \bullet 10^a , \quad (2)$$

The new symbols used have the following definitions:

β'=heating rate nearest the midpoint of the experimental heating rate, 5 K/min

E_r=refined activation energy

a=approximation integral from the Numerical Integration Constants table.[19]

The results of these calculations are showed in the Table 1.

The average value for E_r was calculated inside the range of ±10% and for $R^2 \geq 0.95$ only, in the same time. The correlation coefficient-R^2 is a statistical measure of how well the regression line approximates the points of co-ordinates 1/T, logβ for a constant conversion. The $R^2 \geq 0.95$ describes a good fitting of the experimental data with linear model.

The precision of the E_r calculation depends of the quality of the linear fit for the points of constant conversion with coordinates 1/T, logβ, as the slope(Δ(log β)/ Δ(1/T)) for their regression line is one of the factors in Eq. 1, so the correlation coefficient R^2 describes also the precision for the found E_r values. The values of the E_r for empty cells of Table 1 cannot be calculated as the corresponding values for E/RT_c were higher than 60, the maxim value in the Numerical Integration Constants table.

Table 1

The values of activation energy-E_r and lnA and the averages their values for all synthesized compounds

α , %	H_3PW			Cs_1H_2PW			Cs_2H_1PW			$Cs_{2.5}H_{0.5}PW$		
	Er, kJ/mol	**R^2**	**lnA**	**Er, kJ/mol**	**R^2**	**lnA**	**Er, kJ/mol**	**R^2**	**lnA**	**Er, kJ/mol**	**R^2**	**lnA**
5	241.5	0.996	54.84	289.4	0.895	66.08	200.8	0.968	48.74	188.8	0.940	45.64
10	259.4	0.996	57.58	292.6	0.964	65.76	247.5	0.982	57.62	199.7	0.987	47.36
15	265.1	0.995	56.73	275.7	0.989	62.10	247.2	0.969	57.02	216.8	0.992	50.86
20	264.6	0.994	58.31	281.2	0.983	62.40	263.8	0.992	60.39	224.1	0.998	50.10
25	269.5	0.994	58.54	282.1	0.992	62.65	272.3	0.998	61.66	224.9	0.999	50.35
30	271.3	0.992	58.75	274.2	0.989	60.81	260.1	0.999	58.79	232.3	0.998	51.58
35	272.9	0.989	57.89	261.9	0.996	57.92	271.3	0.999	61.02	238.2	0.997	51.75
40	272.5	0.975	58.06	262.3	0.996	58.09	256.2	0.992	57.08	249.9	0.998	53.96
45	284.0	0.983	59.22	267.4	0.994	58.23	264.7	0.999	58.25	247.0	0.998	53.09
50	284.8	0.983	59.37	271.2	0.998	58.36	260.8	0.997	57.37	249.3	0.998	53.22
55	292.9	0.984	59.48	267.8	0.997	57.48	259.5	0.999	57.51	253.4	0.997	53.35
60	297.8	0.979	60.64	274.6	0.997	58.63	247.3	0.998	54.56	257.8	0.998	53.47
65	301.7	0.979	60.77	284.3	0.999	59.78	247.6	0.999	54.70	265.0	0.997	54.63

Table 1 (continued)

70	304.1	0.979	60.90	298.4	0.994	61.95	251.9	0.999	54.82	271.2	0.991	54.74
75	297.5	0.976	60.02	314.5	0.997	64.11	250.1	0.998	53.92	285.2	0.990	56.92
80	325.7	0.971	63.20	354.2	0.994	70.36	257.0	0.998	55.09	301.5	0.998	59.10
85	391.4	0.948	73.55	-	-	-	291.7	0.996	60.35	304.8	0.988	58.21
90	-	-	-	-	-	-	371.9	0.960	71.72	331.4	0.991	62.49
Av. val.	**282±23 10≤α≥75**		**58.5 ±2.5**	**280±18 10≤α≥70**		**61.5 ±4.5**	**260±13 10≤α≥80**		**58±4**	**248±24 15≤α≥70**		**52.5±2.5**

The average values of E_r from Table 1 are very close for the H_3PW and CsH_2PW_{12}, which could be a heterogeneous mixture of 2:1 between the H_3PW and the Cs_3PW, but with similar secondary structure for the H_3PW of mixture and the H_3PW in bulk.

The activation energy for Cs_2HPW and $Cs_{2.5}H_{0.5}PW$, which could be a heterogeneous mixture of 1:2, respectively of 1:5, between H_3PW and Cs_3PW, shows lower values, possible as result of the H_3PW spread on the Cs_3PW crystalline aggregate surface and of the lower degree of crystallization as consequence.

The calculation of the H_3PW layers on a model of the spherical or cubic aggregates, with a core of Cs_3PW crystallites covered of H_3PW molecules as outer layers, gives: 7 layers of H_3PW for CsH_2PW, 2.3 layers of H_3PW for Cs_2HPW and 1 layer of H_3PW for $Cs_{2.5}H_{0.5}PW$ and the model was confirmed of XPS measurement for Cs concentration.[31] It could be supposed: - the existence of a high number of H_3PW crystallites in the case of 7 layers of H_3PW and as consequence, the same activation energy as the H_3PW in bulk, -a lower number of H_3PW crystallites in the case of 2.3 layers of H_3PW and a very low number of H_3PW crystallites in the case of monolayer coverage, with the consequences of lower activation energy, especially for the last situation.

CONCLUSIONS

The main thermal decomposition processes of the $H_3PW{\cdot}6H_2O$ and its acidic salts, $Cs_x H_{3-x}PW{\cdot}yH_2O$, consist of the removal of: physical adsorbed water (especially for the salt with higher specific surface area), crystallization water and constitutional water. The crystallization water loss occurs in two steps: the first step corresponds to the loss of the water molecules bound by hydrogen weak bond; the second step corresponds to removal of the water molecule of $H_5O_2^+$. The physical adsorbed water was removed at a temperature little lower than the temperature for the first step of crystallization water loss.

After decomposition, the process of WO_3 crystallization is accompanied by exothermal effects on DTA curves. The increasing intensities of DTA peaks with the heating rate and their decreasing with the increase of the Cs content was put in evidence.

The constitutional water loss could be assigned to H_3PW molecules if the $Cs_x H_{3-x}PW$ are heterogeneous mixture: $(1\text{-}x/3)H_3PW+Cs_x[PW]_{x/3}$, according to FTIR and XRD results for heated samples at 873 K: (a) the presence of specific IR bands for KUs in the IR spectra for the all studied salts and their disappearance from the $H_3PW{\cdot}6H_2O$ spectrum; (b) the lacunary Keggin structure formation by one oxygen atom removal and the P-O band splitting as result of lower symmetry of the central atom (P) were not evidenced in FTIR spectra; (c) the presence of the reflections corresponding to cubic secondary structure of KUs arrangements together with the characteristic reflections of WO_3 from the XRD spectra of the acidic salts and only the presence of characteristic reflections to WO_3 in XRD spectrum of $H_3PW{\cdot}6H_2O$ have been evidenced.

The average values of activation energy are close for the H_3PW and CsH_2PW_{12}, which could be a 2:1 heterogeneous mixture between the H_3PW and the Cs_3PW, but with similar secondary structure for the H_3PW of mixture and the H_3PW in bulk.

The activation energy for Cs_2HPW and $Cs_{2.5}H_{0.5}PW$, which could be a 1:2 and 1:5 heterogeneous mixture respectively, between H_3PW and Cs_3PW, shows lower values, possible as a result of their microstructure which consists of Cs_3PW crystalline aggregate covered of H_3PW layers and as a consequence of the lower degree of crystallization for H_3PW.

The activation energy values calculated in respect of Standard Test Method for Decomposition Kinetics by Thermogravimetry are

reliable and can be used to calculate thermal endurance and to estimate the lifetime of the compounds at a certain temperature.

Acknoledgements: Research was partially supported by Roumanian Academy Research Programme carried out by Institute of Chemistry of Timişoara.

REFERENCES

1. F. Cavani, *Catal. Today*, **1998**, *41*, 73-86.
2. M. Misono, *Catal. Rev.,* **1987**, *29*, 269-321.
3. M. Misono, *Chem. Commun.,* **2001**, 1141-1152.
4. J. B. Monagle and J. B. Moffat, *J. Catal.,* **1985,** *91*, 132-141.
5. Y. Saito, P. N. Park, H. Niiyama and E. Echigoya, *J. Catal.,* **1985,** *95,* 49-56.
6. K.Y. Lee, T. Aray, S. Nakata, S.Asaoka, T. Okuhara and M. Misono, *J. Am. Chem. Soc.,* **1992**, *114*, 2836-2842.
7. D. Varisli, T. Dogu and G. Dogu, *Chem. Eng. Sci.,* **2007,** *62*, 5349-5352.
8. L. Matachowski, A. Zięba, M. Zembala and A. Drelinkiewicz, *Catal. Lett.,* **2009,** *133,* DOI10.1007/ s10562-009-0149-y.
9. Yan Lin, Shuzo Tanaka, *Appl. Microbiol. Biotechnol.*. **2006,** *69*, 627–642;
10. K. Narasimharao*,* D.R. Brown, A.F. Lee, A.D. Newman, P.F. Siril, S.J. Tavener and K. Wilson, *J. Catal*., **2007**, *248*, 226-234.
11. P. Morin, B. Hamad, G. Sapaly, M.G. Carneiro Rocha, P.G. Pries de Oliveira, W.A. Gonzalez, E. Andrade Sales and N. Essayem, *Appl. Catal. A: General,* **2007**, *330*, 69-76.
12. P. Morin, B. Hamad, G. Sapaly, M.G. Carneiro Rocha, P.G. Pries de Oliveira, W.A. Gonzalez, E. Andrade Sales and N. Essayem, *Catal. Comunn.,* **2008,** *10*, 92-97.
13. A. Bielański, A. Lubańska, A. Micek-Ilnicka and J. Pożniczek*, Coord. Chem. Rev.,* **2005**, *249*, 2222-2231.
14. S. Berndt, D. Herein, F. Zemlin, E. Beckmann, G. Weinberg, G. Schütze, G. Mestl and R. Schlögl, *Ber. Bunsenges. Phys. Chem.,* **1998**, *102*, 763-774.
15. T. Okuhara, and T. Nakato, *Catal. Surv. Japan,* **1998**, *2*, 31-44.
16. T. Okuhara, H. Watanabe, T. Nishimura, K. Inumaru and M. Misono, *Chem. Mater.,* **2000**, *12*, 2230-2238.
17. M. Misono, *Chem. Commun.,* **2001**, 1141-1152.
18. T. Okuhara , *Appl. Catal. A: General,* **2003**, *256*, 213-224.
19. ASTM, E 1641-64, 1-7.
20. J. C. Bailar, *Inorg. Synth.,* **1939**, *1*, 132-133.
21. M. Misono, N. Mizuno, K. Katamura, A. Kasai, Y. Konishi, K. Sakata, T. Okuhara, and Y. Yoneda, *Bul. Chem. Soc. Jpn*., **1982**, 55, 400-406
22. C. Rocchiccioli-Deltcheff, M. Fournier, R. Franck and R. Thouvenot, *Inorg. Chem.,* **1983**, *22*, 207-216.
23. N. Essayem, A. Holmqvist, P.Y.Gayraud, J.C. Vedrine and Y.B. Taarit, *J. Catal.,* **2001**, *197*, 273-280.
24. J. G. Highfield and J.B. Moffat, *J. Catal.,* **1984**, *88*, 177-187.
25. G. M. Brown, M.-R. Noe-Spirlet, W.A. Busing and H.A. Levy, *Acta cryst. B,* **1977**, *33,* 1038-1046.
26. P.A. Jalil, M. Faiz, N. Tabet, N.M. Hamdan and Z. Hussain, *J. Catal.,* **2003**, *217*, 292-297.
27. A. Kremenović, A. Spasojević-de Biré, R. Dimitrijević, P. Sciau and U.B. Mioć, *Solid State Ionics,* **2000**, *132*, 39-53.
28. K. Okumura, K. Yamashita, K. Yamada and M. Niwa, *J. Catal.,* **2007**, *245*, 75-83.
29. H. Yang , F. Shang , L. Gao and H. Han, *Appl. Surf. Sci.,* **2007**, *253*, 5553–5557.
30. K. Nowinska, A. Waclaw, M. Sopa and M. Klal, *Catal. Lett.,* **2002**, *78*, 347-352
31. V. Sasca, O. Verdes, L. Avram, A. Popa, A. Erdőhelyi and A. Oszko, Data **2010** in manuscript.